Vapor pressures and vapor phase compositions of choline chloride urea and choline chloride ethylene glycol deep eutectic solvents from molecular simulation

Hirad S. Salehi,[1] (iD) H. Mert Polat,[1,2,3] (iD) Frédérick de Meyer,[2,3] (iD) Céline Houriez,[3] Christophe Coquelet,[3] (iD) Thijs J. H. Vlugt,[1] (iD) and Othonas A. Moultos[1,a)] (iD)

AFFILIATIONS

[1] Engineering Thermodynamics, Process & Energy Department, Faculty of Mechanical, Maritime and Materials Engineering, Delft University of Technology, Leeghwaterstraat 39, 2628CB Delft, The Netherlands
[2] CCUS and Acid Gas Entity, Liquefied Natural Gas Department, Exploration Production, Total Energies S.E., 92078 Paris, France
[3] CTP - Centre of Thermodynamics of Processes, Mines ParisTech, PSL University, 35 rue Saint Honoré, 77305 Fontainebleau, France

Note: This paper is part of the 2021 JCP Emerging Investigators Special Collection.
a) Author to whom correspondence should be addressed: O.Moultos@tudelft.nl

ABSTRACT

Despite the widespread acknowledgment that deep eutectic solvents (DESs) have negligible vapor pressures, very few studies in which the vapor pressures of these solvents are measured or computed are available. Similarly, the vapor phase composition is known for only a few DESs. In this study, for the first time, the vapor pressures and vapor phase compositions of choline chloride urea (ChClU) and choline chloride ethylene glycol (ChClEg) DESs are computed using Monte Carlo simulations. The partial pressures of the DES components were obtained from liquid and vapor phase excess Gibbs energies, computed using thermodynamic integration. The enthalpies of vaporization were computed from the obtained vapor pressures, and the results were in reasonable agreement with the few available experimental data in the literature. It was found that the vapor phases of both DESs were dominated by the most volatile component (hydrogen bond donor, HBD, i.e., urea or ethylene glycol), i.e., 100% HBD in ChClEg and 88%–93% HBD in ChClU. Higher vapor pressures were observed for ChClEg compared to ChClU due to the higher volatility of ethylene glycol compared to urea. The influence of the liquid composition of the DESs on the computed properties was studied by considering different mole fractions (i.e., 0.6, 0.67, and 0.75) of the HBD. Except for the partial pressure of ethylene glycol in ChClEg, all the computed partial pressures and enthalpies of vaporization showed insensitivity toward the liquid composition. The activity coefficient of ethylene glycol in ChClEg was computed at different liquid phase mole fractions, showing negative deviations from Raoult's law.

Published under an exclusive license by AIP Publishing. https://doi.org/10.1063/5.0062408

I. INTRODUCTION

Deep eutectic solvents (DESs) are designer solvent mixtures that have attracted the attention of the scientific community due to potentially promising properties, such as good solvation for a variety of solute molecules, non-flammability, biodegradability, and inexpensive and easy preparation.[1–7] DESs are often categorized into several types based on the nature of the precursor components.[2,8] The most commonly studied DESs are composed of hydrogen bond acceptors (HBAs), such as choline chloride, and hydrogen bond donors (HBD), such as urea. The chemical structures of these starting compounds, as well as the mixing ratio, have a significant influence on the thermo-physical properties of DESs[1] and can therefore be tuned toward specific applications. DESs are often marked by a large melting point depression upon mixing and an extensive hydrogen bond network,[2,7] although these

characteristics are debated.[9] Recently, a special issue of the Journal of Chemical Physics titled "Chemical Physics of Deep Eutectic Solvents" was launched, to which the reader is referred for more information on DESs.[10–19]

DESs and ionic liquids (ILs) are often regarded as superior solvents compared to volatile organic compounds (VOCs) due to a negligible vapor pressure at room temperature.[2,5,6,20] Such a low vapor pressure would limit the emission and loss of the DESs into the atmosphere and may facilitate the removal of solutes from DESs by distillation.[21] Despite the widespread acknowledgment of low vapor pressures of DESs, very few studies reporting measurements of the vapor pressures of these solvents are available in the literature.[21–28] Wu *et al.*[27] measured, for the first time, the vapor pressures of aqueous solutions of choline chloride-based DESs, with DES mole fractions in the range of 0.035–0.45. Shahbaz *et al.*[22] measured the vapor pressures of pure DESs, composed of a variety of HBA and HBD components, by thermogravimetric analysis (TGA). The authors found that the vapor pressures of the DESs based on urea are lower than those of DESs containing glycerol (with the same HBA component). Moreover, the measured vapor pressures of glycerol-based DESs were lower than the vapor pressure of pure glycerol, indicating stronger intermolecular interactions within the DES mixtures. It was further concluded that the vapor pressures of DESs are higher than those of commonly studied ILs. Ravula *et al.*[23] measured the vapor pressures of several DESs (along with some ILs and molecular solvents) in a wide range of temperatures using the TGA method. While the authors found a reasonable agreement for the vapor pressure data of choline chloride glycerol with those of Shahbaz *et al.*,[22] the obtained vapor pressures of choline chloride urea were higher than those reported by Shahbaz *et al.*[22] by an order of magnitude.

As DESs are mixtures, the DES components can, in principle, vaporize separately from the liquid phase into the vapor phase, thereby changing the composition of the liquid phase. The extent of this change in the liquid phase composition depends on the amounts of the liquid and vapor phases and the evaporation rate. The first characterization of the vapor phase composition of DESs was performed by Dietz *et al.*,[21] where the authors measured the partial pressures of the components of several hydrophobic DESs, using headspace gas chromatography-mass spectrometry (HS-GC-MS). The vapor pressure and composition were shown to be dominated by the most volatile component of the DESs. The obtained vapor pressures indicated a lower volatility for the hydrophobic DESs compared to common organic solvents and a higher volatility compared to common ILs. The authors also showed that the HS-GC-MS method is more reliable than TGA for the determination of the vapor pressures of DESs. HS-GC-MS has been used in a few other publications to determine the vapor pressure and composition of DESs.[24,25,28] Lima *et al.*[25] measured the partial pressures of sulfolane-based DESs at various concentrations of the HBD component (sulfolane). It was demonstrated that the vapor phases of these DESs are dominated by sulfolane as the more volatile component. Consistently, an increase in the salt concentration (decrease in the sulfolane concentration) resulted in lower vapor pressures. To the best of our knowledge, no other studies exist in the literature that report the vapor phase composition of DESs.

The small magnitude of vapor pressure and the hygroscopicity of DESs are factors that make precise measurements of the vapor pressures of these materials challenging.[22,23] This is reflected by the scarcity of such data and the disparities between few available experimental vapor pressure data from different sources.[22,23] Therefore, computational and modeling tools can play an important role in the prediction and understanding of the vapor–liquid equilibrium of DESs, particularly in cases where experimental data are unavailable, scarce, or inconsistent. Nevertheless, very few modeling works are available in the literature that report computations of the vapor phase properties of DESs or establish a relationship between these properties and the liquid structure of DESs. The PC-SAFT equation of state[29] and COSMO-RS[30] have been used in a few studies to model the vapor pressures of DESs.[21,24,25,28,31] Molecular Dynamics (MD) simulations have been performed to compute solubility parameters and enthalpies of vaporization of choline chloride-based DESs.[32,33] In the study by Salehi *et al.*,[32] it was concluded, based on the computed vaporization enthalpies, that the HBD component (the most volatile component) likely dominates the vapor phase of choline chloride-based DESs, although no precise vapor composition was provided. In the MD study by Ferreira *et al.*,[33] next to HBD molecules, DES clusters, composed of two HBD molecules and one HBA molecule, were deemed likely to appear in the vapor phase of choline chloride ethylene glycol.

In this work, Monte Carlo (MC) simulations were performed in combination with thermodynamic integration to compute the excess Gibbs energies and thereby the vapor pressures of choline chloride ethylene glycol (ChClEg) and choline chloride urea (ChClU) DESs. In these DESs, the choline chloride salt is the HBA component, while urea and ethylene glycol are the HBD components. ChClU and ChClEg were chosen in this work as these (and choline chloride-based DESs in general) are commonly studied DESs with a wide range of potential applications.[2,7] Furthermore, unlike many other DESs, well-established classical force fields are available for ChClU and ChClEg.[33–36] Here, the partial pressures and vapor phase compositions were obtained for ChClU and ChClEg from the computed excess Gibbs energies. The enthalpies of vaporization were calculated from the vapor pressure data using the Clausius–Clapeyron relation. The computed enthalpies of vaporization and vapor pressures were in reasonable agreement with experimental data, although the inconsistencies between the experimental data made the comparisons difficult. The activity coefficients of ethylene glycol in ChClEg were computed in order to quantify the non-ideality of the mixture. To investigate the influence of the liquid phase composition on the computed properties, three different HBA:HBD molar ratios, i.e., 1:1.5, 1:2 (the eutectic ratio of both DESs), and 1:3, were considered in the simulations of each DES. The relatively small standard deviations in the calculated liquid phase excess Gibbs energies (average, ~1.5 kJ mol^{-1}) and partial pressures (average, ~174 Pa) demonstrated the high reliability and precision of the thermodynamic integration method for such computations.

This paper is organized as follows: In Sec. II, the simulation details and computational methods are discussed. Subsequently, the simulation results are discussed and, when possible, compared with experimental data from the literature. Finally, conclusions are provided regarding the computation of vapor pressures and vapor phase compositions of DESs from MC simulations.

II. COMPUTATIONAL METHODS

The all-atom non-polarizable Generalized AMBER Force Field (GAFF)[37] was used to model both ChClEg and ChClU. It has been shown that this force field can accurately predict the thermodynamic, structural, and transport properties of ChClEg and ChClU, as well as other DESs.[34,35,38] Bonded interactions, including bond-bending and torsion, and non-bonded interactions, consisting of Lennard-Jones (LJ) and electrostatic potentials, were used to account for the intra- and intermolecular interactions. All bond lengths were kept fixed at equilibrium lengths, and improper torsions were not taken into account. It has been shown that bond rigidity and the exclusion of improper torsions do not have a considerable influence on the computed densities and liquid structures of ChClEg and ChClU.[39] All partial charges were taken from the studies by Perkins et al.,[34,35] in which the charges were derived at the $HF/6 - 31G^*$ level of theory using the restrained electrostatic potential (RESP) method.[40,41] The charges of ions (choline and chloride) were scaled by 0.9 and 0.8 in ChClEg and ChClU, respectively, to enhance the agreement of the simulation results with experimental data.[34,35] To prevent atomic overlaps, the values $\varepsilon/k_B = 0.5$ K (where k_B is the Boltzmann constant) and $\sigma = 0.1$ Å were used as the LJ parameters of unprotected hydroxyl hydrogen atoms.[42] Scaling factors of 0.5 and 0.833 were used for the 1–4 intramolecular LJ and electrostatic energies, respectively.[43] The structures and force field parameters of all the molecules are presented in the supplementary material. The Ewald summation method, with a relative precision of 10^{-6}, was used to calculate the long-range electrostatic energies.[44,45] The LJ and short-range electrostatic potentials were truncated at a cutoff radius of 10.0 Å. Analytic tail corrections were used to account for the long-range contributions of the LJ energies.[46] The Lorentz–Berthelot mixing rules were used to calculate the LJ interactions between non-identical atom-types.[46] It is important to note that in our previous MC simulation study,[39] the force field parameters of ChClU and ChClEg (with a molar ratio of 1:2) were validated with experimental data and MD simulation results.[34,35,38]

All simulations were performed using the open-source Brick-CFCMC software,[47–49] which applies the continuous fractional component Monte Carlo (CFCMC) method[49–54] for molecule insertions. In this method, an additional "fractional" molecule exists in the simulation box, for which the interactions with other molecules (referred to as "whole" molecules) are scaled by a scaling parameter $\lambda \in [0, 1]$. A detailed description of this method and its implementation in Brick-CFCMC can be found in our previous publications.[39,48,49,53,55–57] To compute the average liquid phase densities and excess Gibbs energies, simulations were performed in the isobaric–isothermal (NPT) ensemble at a pressure of 1 bar and different temperatures. The simulations of ChClU were carried out at 393 and 433 K. For ChClEg, the simulations were performed at 353 and 393 K. For each DES, three sets of simulations were performed at different HBA:HBD molar ratios, i.e., 1:1.5, 1:2 (eutectic ratio), and 1:3. The numbers of molecules used in the simulations at each molar ratio are listed in Table S10 of the supplementary material. Each molar ratio corresponds to a certain mole fraction of the HBD component (urea or ethylene glycol) in the mixture, which is defined as

$$x_{HBD} = \frac{N_{HBD}}{N_{HBD} + N_{ChCl}}, \tag{1}$$

where N_{HBD} and N_{ChCl} are the number of molecules of the HBD component (urea or ethylene glycol) and the number of choline chloride ion pairs (half of the total number of ions of the HBA), respectively. Therefore, the HBA:HBD molar ratios (N_{HBA}/N_{HBD}) of 1:1.5, 1:2, and 1:3 correspond to the HBD mole fractions of 0.6, 0.67, and 0.75. The mole fraction of choline chloride in the DESs can be calculated as $x_{ChCl} = 1 - x_{HBD}$.

For each combination of temperature and molar ratio, two separate sets of simulations were carried out, i.e., one containing an additional fractional molecule of the HBD and one containing an additional fractional "group"[47] of the HBA, as vaporizing entities. The fractional group of the HBA consisted of a single fractional molecule/ion of chloride and a single fractional molecule/ion of choline. The grouping of the choline and chloride ions into a single HBA component was carried out in accordance with experimental and computational studies of ILs, in which the vapor phase has been demonstrated to mostly consist of isolated ion pairs rather than single ions or large clusters.[58–63] Thermodynamic integration was used to compute the excess Gibbs energy of each DES component (HBA or HBD) in the NPT ensemble, ΔG_{NPT}^{ex}, according to[44]

$$\Delta G_{NPT}^{ex} = \Delta A_{NVT}^{ex} = \int_0^1 \left\langle \frac{\partial U}{\partial \lambda} \right\rangle d\lambda, \tag{2}$$

where ΔA_{NVT}^{ex} is the excess Helmholtz energy of that component, computed in the canonical (NVT) ensemble; λ is the scaling parameter of the fractional molecule/group of the DES component; U is the potential energy of the system; and the brackets $\langle \cdots \rangle$ denote an ensemble average. We used 50 values of λ, evenly distributed in the range (0,1), to compute the integral in Eq. (2). For each value of λ, a separate simulation was carried out (λ was fixed during each simulation), from which the ensemble average in Eq. (2) was computed. Using Brick-CFCMC, the values of $\partial U/\partial \lambda$ are automatically computed for all non-bonded interactions, including the Ewald summation.[48] To enhance the accuracy of the integration in Eq. (2), a cubic spline was fit to $\langle \partial U/\partial \lambda \rangle$ as a function of λ.

All liquid phase simulations were started from well-equilibrated (in terms of the density and total energy) initial configurations at the respective temperatures. 3×10^5 additional equilibration MC cycles and 4×10^5 production MC cycles were used for each value of λ. Each MC cycle consisted of various trial moves (as many as the number of molecules), selected with fixed probabilities, which thermalized the system. These trial moves included translations, rotations, volume changes, changes in the internal configuration of molecules (angles and dihedrals), reinsertions of the fractional molecule at a random position in the box, and exchanges of the identity of the fractional molecule with a randomly selected whole molecule. No trial moves that attempt to change λ were performed, as the value of λ was fixed in each simulation. For each data point, 3–5 independent runs were carried out, over which the mean and standard deviation values were calculated. Two separate parameters, i.e., λ_{LJ} and λ_{el}, were used to independently scale the LJ and electrostatic interactions of the fractional molecules/groups, respectively, using the following scheme: between $\lambda = 0.0$ and $\lambda = 0.5$, the LJ interactions were scaled using λ_{LJ}, while the electrostatic interactions remained fully switched-off ($\lambda_{el} = 0.0$), and between $\lambda = 0.5$ and $\lambda = 1.0$, the electrostatic interactions were scaled using λ_{el}, while the LJ

interactions remained fully switched-on ($\lambda_{LJ} = 1$). The relation between the LJ and electrostatic scaling parameters and the overall scaling parameter of the fractional molecule/group (λ) is chosen such that atomic overlaps are avoided and is described in Ref. 48. The scaling of the LJ and electrostatic energies with λ_{LJ} and λ_{el} (and the optimal scaling parameters) is discussed in our previous study,[39,48] and the exact functional forms for the scaling are provided in the supplementary material of Ref. 48.

It is important to note that in principle, the excess Gibbs energy (the excess chemical potential) of a fractional molecule can also be computed from the probability distribution of λ in a single simulation, where a random walk is carried out in λ-space. This method has been successfully used in previous works by our group.[39,55,57,64,65] Although this method is accurate and reliable for small fractional molecules with relatively weak interactions, e.g., CO_2, the sampling of λ-space becomes increasingly challenging and inefficient when the size and the strength of interaction of the fractional molecule become larger (e.g., DES components), resulting in large uncertainties in the computed excess Gibbs energies. Therefore, thermodynamic integration was used in this work as an alternative method to compute the excess Gibbs energies of DES components.

The vapor phase of the DESs was assumed to be an ideal gas composed of isolated, non-interacting molecules of the HBD component (urea or ethylene glycol) and isolated, non-interacting choline chloride (HBA component) ion pairs. Due to the low vapor pressures of the DESs,[22,23] the ideal gas approximation of the vapor phase is reasonable. The assumption of choline chloride existing in the vapor phase as ion pairs has also been used in the simulations of ILs,[60,66] and other salts, e.g., NaCl,[67] and is consistent with experimental observations of the vapor phase of ILs,[58,61,63] as discussed earlier. Test simulations were carried out in the gas phase at various box sizes to examine whether dimer formation was favorable for the HBD molecules. No considerable dimer formation was found in the simulations, reinforcing the assumption that the HBD molecules exist as monomers in the gas phase. Using the equality of chemical potentials in the liquid and vapor phases, the partial pressure of the HBD component (urea or ethylene glycol) in the corresponding DES was computed as[55,67]

$$P_{HBD} = \frac{N_{HBD} k_B T}{V} \exp\left[\frac{\Delta G_{HBD}^{ex,l} - \frac{V}{N_{HBD}} P^0}{k_B T}\right], \quad (3)$$

where N_{HBD} is the number of HBD molecules in the DES liquid phase; k_B is the Boltzmann constant; T is the temperature; V is the volume of the liquid phase simulation box; $\Delta G_{HBD}^{ex,l}$ is the liquid phase excess Gibbs energy of the HBD, computed from thermodynamic integration [Eq. (2)]; and $P^0 = 1$ bar is the reference state pressure. In Eq. (3), the partial molar volume of the HBD is approximated by V/N_{HBD} (V and N_{HBD} are the liquid phase volume of the DES and the number of HBD molecules, respectively), assuming a negligible excess volume of the liquid phase of the DES, as supported by the MD simulation results of Celebi et al.[14] for ChClU. In principle, the excess and mixing properties, e.g., volume and enthalpy, can be computed from Kirkwood–Buff integrals,[68] although such computations are beyond the scope of this work. In the derivation of Eq. (3), it was further assumed that the vapor pressure of the DES is small compared to the reference state pressure (P^0) of 1 bar. Considering the low vapor pressures of DESs as reported from measurements,[21–25,28]

this is a reasonable assumption. The detailed derivation of Eq. (3) is provided in the supplementary material.

To account for the interaction between the choline cation and chloride anion of each isolated ion pair in the vapor phase, simulations were performed for the computation of the excess Gibbs energy of an isolated choline chloride pair. The vapor phase simulations of choline chloride were carried out in the NVT ensemble and consisted of a single fractional group of choline chloride, i.e., one fractional molecule/ion of choline and one fractional molecule/ion of chloride. From the equality of liquid and vapor phase chemical potentials, the partial pressure of choline chloride in each DES was computed according to[67]

$$P_{ChCl} = \frac{N_{ChCl} k_B T}{V} \exp\left[\frac{\Delta G_{ChCl}^{ex,l} - \Delta G_{ChCl}^{ex,v} - \frac{V}{N_{ChCl}} P^0}{2 k_B T}\right], \quad (4)$$

where N_{ChCl} is the number of choline chloride ion pairs (half of the total number of ions) in the DES liquid phase and $\Delta G_{ChCl}^{ex,l}$ and $\Delta G_{ChCl}^{ex,v}$ are the excess Gibbs energies of choline chloride in the liquid phase and vapor phase, respectively. The term $\Delta G_{ChCl}^{ex,v}$ in Eq. (4) was computed as[67]

$$\Delta G_{ChCl}^{ex,v} = \Delta A_{NV^*T}^{ex} - k_B T - k_B T \ln \frac{V^* P^0}{k_B T}, \quad (5)$$

where V^* is the volume of the gas phase simulation box and $\Delta A_{NV^*T}^{ex}$ is the excess Helmholtz energy of choline chloride at the (fixed) gas phase simulation volume (V^*), computed from thermodynamic integration [Eq. (2)]. Similar to the study by Kussainova et al.,[67] the value of $\Delta G_{ChCl}^{ex,v}$ was computed at multiple simulation volumes V^* (35 to 100 Å), and the results were extrapolated (as a function of the inverse of the box size) to infinite volume in order to correct for the effects of long-range Ewald and tail correction energies between the molecules and their periodic images. Similar to Eq. (3), in Eq. (4), the partial molar volume of choline chloride is approximated by V/N_{ChCl} (V and N_{ChCl} are the liquid phase volume of the DES and the number of choline chloride ion pairs, respectively), and the vapor pressure of the DES is assumed small compared to the reference state pressure (1 bar). The detailed derivations of Eqs. (4) and (5) are presented in the supplementary material and are based on the derivation by Kussainova et al.[67]

From the computed partial pressures of the DES components [Eqs. (3) and (4)], the vapor pressures of the DES mixtures were obtained as

$$P^v = P_{HBD} + P_{ChCl}, \quad (6)$$

and the vapor phase mole fraction of component i (HBD or choline chloride) was calculated as $y_i = P_i/P^v$. In a few other publications, the vapor pressure of a DES (P^v) is referred to as the "total vapor pressure."[21,24,25,28]

To investigate the non-ideality of the ChClEg mixture, the activity coefficient of ethylene glycol, γ_{eg}, was computed according to the modified Raoult law[69] as follows:

$$\gamma_{eg} = \frac{P_{eg}}{x_{eg} P_{eg}^{sat}}, \quad (7)$$

where P_{eg} is the computed partial pressure of ethylene glycol [from Eq. (3)] in the vapor phase of ChClEg, x_{eg} is the mole fraction of

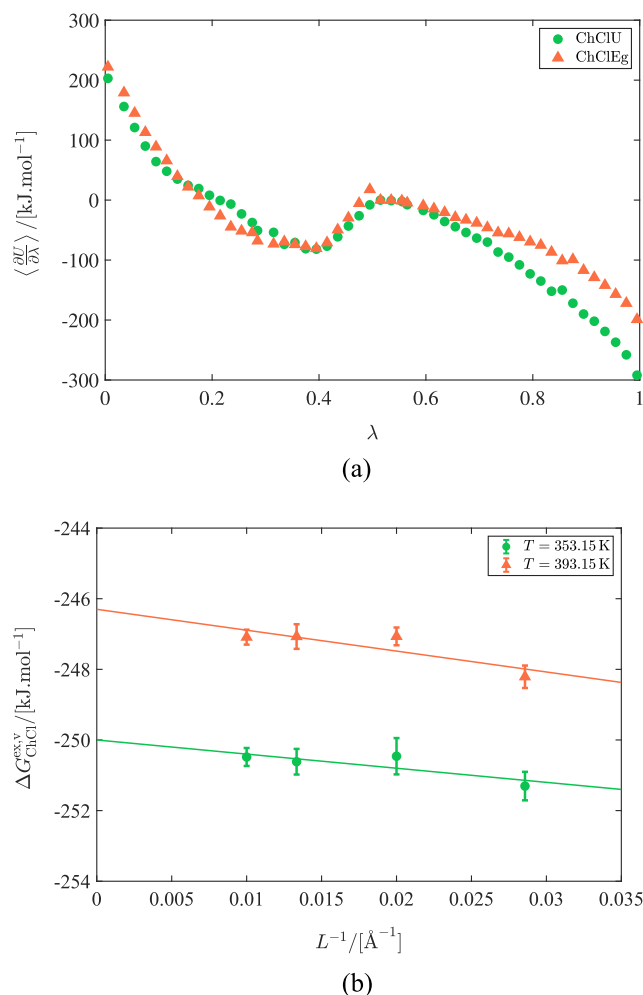ethylene glycol in the liquid phase of ChClEg [Eq. (1)], and P_{eg}^{sat} is the saturated vapor pressure of pure ethylene glycol. To calculate P_{eg}^{sat}, liquid phase simulations were carried out for pure ethylene glycol, and the excess Gibbs energy was obtained at 353 K and 1 bar (in the *NPT* ensemble) from thermodynamic integration according to Eq. (2). The vapor pressure of pure ethylene glycol was calculated using Eq. (3), assuming an ideal gas phase of isolated molecules. The same force field parameters were used for pure ethylene glycol as in the simulations of ChClEg. The activity coefficient calculations were not performed for choline chloride due to the fact that pure choline chloride is a solid (with a melting point of ~575 K) at the simulated temperatures. Urea has an experimental melting point of ~406 K, which is lower than the simulated temperature of 433 K. However, test MC simulations of pure urea (using the same force field parameters as in ChClU) showed a glassy state at 433 K, with limited changes in the configuration of the system. Furthermore, a density of ~1400 kg m^{-3} was obtained at 433 K and 1 bar, which is considerably larger than the experimental value of ~1335 kg m^{-3} at room temperature and pressure (solid state). Thus, the force field parameters used in this work are likely unsuitable for simulations of pure urea. The activity coefficient was therefore not calculated here for urea in ChClU mixtures.

III. RESULTS AND DISCUSSION

A. Partial pressures and vapor phase compositions

To compute the excess Gibbs energies of HBA and HBD components, the function $\langle \partial U / \partial \lambda \rangle$ was integrated according to Eq. (2). The obtained values of $\langle \partial U / \partial \lambda \rangle$ (averaged over all independent runs), as a function of λ, are presented in Fig. 1(a) for urea in ChClU (at 393 K) and ethylene glycol in ChClEg (at 353 K). Similar figures were obtained for choline chloride in the liquid and gas phase simulations (Fig. S4 in the supplementary material). For the vapor phase of choline chloride, the excess Gibbs energy ($\Delta G_{ChCl}^{ex,v}$) was computed using Eq. (5). To correct for the finite size effects, the obtained data for $\Delta G_{ChCl}^{ex,v}$ were linearly extrapolated to infinite volume, as a function of the inverse of the box size.[67,70] The vapor phase excess Gibbs energies of choline chloride ($\Delta G_{ChCl}^{ex,v}$) in ChClEg as a function of the inverse of the box size are presented in Fig. 1(b), at box sizes of 35, 50, 75, and 100 Å. It can be observed in Fig. 1(b) that at both temperatures, the value of $\Delta G_{ChCl}^{ex,v}$ shows a linear dependence (within the error bars) on the inverse of the box size. The same was observed for the vapor phase excess Gibbs energy of choline chloride in ChClU, as presented in Fig. S5 in the supplementary material.

The computed values for the excess Gibbs energies, partial pressures, and vapor phase mole fractions are listed in Table I for both components of ChClU and ChClEg at a molar ratio of 1:2 (eutectic ratio) and various temperatures. It can be observed that for both ChClU and ChClEg, the liquid phase excess Gibbs energies of choline chloride ($\Delta G_{ChCl}^{ex,l}$) are significantly larger than those of the HBD components ($\Delta G_{HBD}^{ex,l}$), indicating a larger magnitude for the intermolecular interactions of choline chloride in the mixtures. Although partially compensated by $\Delta G_{ChCl}^{ex,v}$, the larger excess Gibbs energies of choline chloride compared to those of the HBD molecules in the DES mixtures resulted in considerably smaller partial pressures for choline chloride (Table I). Additionally, the larger number of HBD molecules in each DES mixture, compared to that

FIG. 1. (a) Average values of the derivative of the total energy with respect to λ, as a function of λ, for urea and ethylene glycol components of ChClU and ChClEg, respectively. (b) Vapor phase excess Gibbs energy of choline chloride in ChClEg as a function of the inverse of the box size at different temperatures. The solid lines in (b) depict the linear fits used for the extrapolation of the values to infinite volume.

of choline chloride, contributes to the larger partial pressure of the HBD component. As can be observed in Table I, the liquid phase excess Gibbs energy of urea in ChClU is larger than that of ethylene glycol in ChClEg, resulting in a considerably larger vapor pressure of ethylene glycol (by two orders of magnitude) compared to urea. This is consistent with the fact that ethylene glycol in pure form is much more volatile than pure urea.[71,72] The absolute values of the liquid and vapor phase excess Gibbs energies of choline chloride in ChClEg are larger than those in ChClU. The differences in the values of $\Delta G_{ChCl}^{ex,l}$, and to some extent the values of $\Delta G_{ChCl}^{ex,l}$, between ChClEg and ChClU are due to the larger values of ionic charges used for choline chloride in ChClEg (± 0.9) compared to those in ChClU (± 0.8). The absolute value of the "net" excess Gibbs energy of choline chloride ($\Delta G_{ChCl}^{ex,l} - \Delta G_{ChCl}^{ex,v}$) is also larger in ChClEg than in ChClU,

TABLE I. Computed liquid phase excess Gibbs energies, vapor phase excess Gibbs energies (only for choline chloride as these values are zero by definition for the HBD components), partial pressures, and vapor phase mole fractions for the HBD component, i.e., urea or ethylene glycol, and choline chloride (HBA component) in ChClU and ChClEg DESs, at various temperatures, from MC simulations. The values in parentheses are the standard deviations to the precision of the last significant digit.

DES	T/(K)	$\Delta G_{HBD}^{ex,l}$/(kJ mol^{-1})	$\Delta G_{ChCl}^{ex,l}$/(kJ mol^{-1})	$\Delta G_{ChCl}^{ex,v}$/(kJ mol^{-1})	P_{HBD}/(Pa)	P_{ChCl}/(Pa)	y_{HBD}	y_{ChCl}
ChClU	393	−51.2 (10)	−299.6 (33)	−186.4 (2)	4.80×10^0 (14)	4.8 (20)$\times 10^{-1}$	0.91 (7)	0.09 (7)
	433	−47.4 (4)	−291.1 (28)	−183.5 (2)	6.0 (6) $\times 10^1$	5.3 (20)	0.92 (6)	0.08 (6)
ChClEg	353	−30.3 (5)	−398.3 (28)	−250.1 (4)	7.9 (13) $\times 10^2$	1.4 (6)$\times 10^{-4}$	1.00 (0)	0.00 (0)
	393	−27.6 (5)	−385.7 (3)	−246.5 (3)	5.6 (8) $\times 10^3$	7.1 (3)$\times 10^{-3}$	1.00 (0)	0.00 (0)

resulting in a much smaller partial pressure for choline chloride in ChClEg.

As can be observed in Table I, the values of the partial pressures of HBD and HBA components are closer to each other in ChClU compared to ChClEg. As a result, the vapor phase of ChClU is composed of finite amounts of both urea (~91% at 353 K) and choline chloride (~9% at 353 K), while the vapor phase of ChClEg is entirely composed of ethylene glycol. As expected, an increase in temperature yields smaller excess Gibbs energies and larger partial pressures for both the HBA and HBD components of ChClU and ChClEg. The computed vapor phase compositions are, however, not significantly affected by temperature (Table I). It is important to note that as no experimental data are available in the literature for the partial pressures and vapor phase compositions of ChClEg and ChClU, no comparisons can be made between the simulation results and experimental measurements. The computed values for the partial pressures and vapor compositions of the DESs, thus, serve as the first estimates for these parameters. It is important to note, however, that vapor phase compositions and partial pressures have been measured and reported in the literature for a few other (mostly hydrophobic) DESs.[21,24,25,28] For instance, the measurements conducted by Dietz et al.[21] indicate the vapor phase mole fractions of the more volatile components of the considered hydrophobic DESs to lie in the range of 0.85–1.00. This is in agreement with the results obtained in the present work, where the vapor phases of ChClEg and ChClU are shown to be dominated by the more volatile component (HBD), although to different extents (Table I).

B. Vapor pressures and enthalpies of vaporization

The vapor pressure of each DES mixture was obtained by summing the computed partial pressures of the HBA and HBD components [Eq. (6)]. The enthalpies of vaporization, ΔH^{vap}, were calculated by correlating the vapor pressures with temperature using the

Clausius–Clapeyron equation[73] as follows:

$$\ln\left(\frac{P^v}{[\text{Pa}]}\right) = -\frac{\Delta H^{vap}}{RT} + C, \quad (8)$$

where C is a constant and the enthalpy of vaporization has been assumed to be temperature independent. Equation (8) has been successfully used to model the vapor pressures of other DESs.[21,25] The calculated vapor pressures and enthalpies of vaporization of ChClU and ChClEg (both with a molar ratio of 1:2) are listed in Table II. The experimental data in the study by Ravula et al.[23] and Shahbaz et al.[22] (denoted as "exp1" and "exp2" in Table II, respectively) are also listed for comparison. The experimental values of the vapor pressures of the DESs at higher temperatures (433 K for ChClU and 393 K for ChClEg) were obtained by extrapolation of the data using Eq. (8). The experimental datasets were well described by Eq. (8), with a correlation coefficient of $R^2 > 0.995$. The quality of the regression could not be evaluated for the simulation results, as the vapor pressures were only computed at two temperatures.

As can be observed in Table II, there is a clear disparity between the two sets of experimental data for ChClU. The data in the study by Ravula et al.[23] indicate considerably larger values for the vapor pressure and enthalpy of vaporization of ChClU, compared to the data in the study by Shahbaz et al.[22] These discrepancies may be related to the difficulty of measuring such low pressures and/or the use of the TGA method, which has been questioned in other studies of DESs.[21] As a result of these inconsistencies, it is difficult to make precise comparisons between the simulation results and the experimental data. It can be observed in Table II that the computed vapor pressure of ChClU at 393 K from the simulations lies between the experimental data but closer to the value reported by Shahbaz et al.[22] Similarly, at 433 K, the computed vapor pressure of ChClU lies between the extrapolated experimental values. It can be observed that the computed enthalpy of vaporization of ChClU is in agreement with the

TABLE II. Computed vapor pressures and enthalpies of vaporization of ChClU and ChClEg DESs at various temperatures, from MC simulations, compared with the experimental data in studies by Ravula et al.[23] (exp1) and Shahbaz et al.[22] (exp2). The values in parentheses are the standard deviations to the precision of the last significant digit.

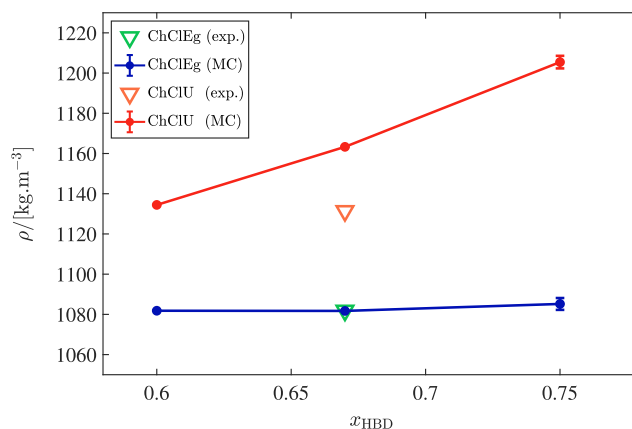| DES	T/(K)	P_{MC}^v/(Pa)	P_{exp1}^v/(Pa)	P_{exp2}^v/(Pa)	ΔH_{MC}^{vap}/(kJ mol^{-1})	ΔH_{exp1}^{vap}/(kJ mol^{-1})	ΔH_{exp2}^{vap}/(kJ mol^{-1})
ChClU	393	5.3 (15)	2.90×10^1	2.9	89.3 (100)	79.0	46.9
	433	6.6 (6) $\times 10^1$	2.80×10^{2a}	1.10×10^{1a}			
ChClEg	353	7.9 (13) $\times 10^2$	9.50×10^1	$\cdots$	56.6 (60)	55.8	$\cdots$
	393	5.6 (8) $\times 10^3$	7.20×10^{2c}	$\cdots$			

^{a}Extrapolated values.

value reported by Ravula *et al.*,[23] while it is considerably larger than the value reported by Shahbaz *et al.*[22] For ChClEg, at both temperatures, the computed vapor pressures are significantly larger than the (extrapolated) experimental values reported by Ravula *et al.*,[23] possibly due to an overestimation of the volatility of ethylene glycol in ChClEg from the simulations (Table I). The computed and experimental enthalpies of vaporization of ChClEg are, however, in excellent agreement. As can be observed in Table II, at 393 K, the computed vapor pressure of ChClEg is considerably larger than that of ChClU (consistent with the experimental data) due to the larger partial pressure of ethylene glycol compared to that of urea (Table I). The computed and experimental vapor pressures of both DESs are much larger than the vapor pressures of commonly studied ILs,[23,74] e.g., 0.93 Pa for $[bmim][BF_4]$ at 503 K.[23]

In our previous study,[32] the enthalpies of vaporization of the HBA and HBD components of several choline chloride-based DESs were computed from average potential energies in separate liquid and gas phase MD simulations. In that study, the enthalpy of vaporization of urea in ChClU (with the same GAFF force field parameters as used here) and of ethylene glycol in ChClEg (using OPLS force field) was obtained as 107 and 73 kJ mol^{-1}, respectively. These values are in agreement with the enthalpies of vaporization of ChClU and ChClEg obtained here (Table II). Such agreement is likely due to the fact that the vapor phase of these DESs is dominated by the HBD component (urea or ethylene glycol). The method of computation of the enthalpies of vaporization based on average liquid and gas phase potential energies (as used in our previous work[32]) has also been employed in other studies to compute the vaporization enthalpies/energies of DESs[33] and ILs.[60,66,75,76] Although this is a simple and computationally cheap method for obtaining the enthalpy of vaporization, it does not provide the vapor pressure and vapor phase composition (in the case of mixtures), as does the method used in the present work. Moreover, for mixtures (e.g., DESs), only the vaporization enthalpies of different components, such as HBA, HBD, or clusters, can be obtained, and the enthalpy of vaporization of the mixture cannot be computed. Neither of these methods, however, provide the configuration of the molecules in the gas phase (e.g., ion pairs, single ions, dimers, or clusters), and this configuration must therefore be assumed in the simulations. In the studies by Rai and Maginn,[59,77] vapor pressures, enthalpies of vaporization, normal boiling points, and critical properties were computed for imidazolium-based ILs using MC simulations in the Gibbs ensemble. This method has the ability to directly determine several vapor–liquid equilibrium properties and provide the gas phase configuration of the molecules. However, these simulations can only be carried out for high temperatures and thus high vapor pressures (~15–300 kPa in the study by Rai and Maginn[59]), where a sufficient number of molecules are transferred to the gas phase at a reasonable system size. For such low vapor pressures as obtained in the present work, a large system size would be necessary for Gibbs ensemble simulations, which would result in a higher computational cost to achieve the same level of precision. The system sizes considered here are relatively small, saving additional computational costs.

C. Effect of liquid composition on DES properties

The densities of the DESs with different mole fractions of the HBD (or HBA:HBD molar ratios) were computed directly from the
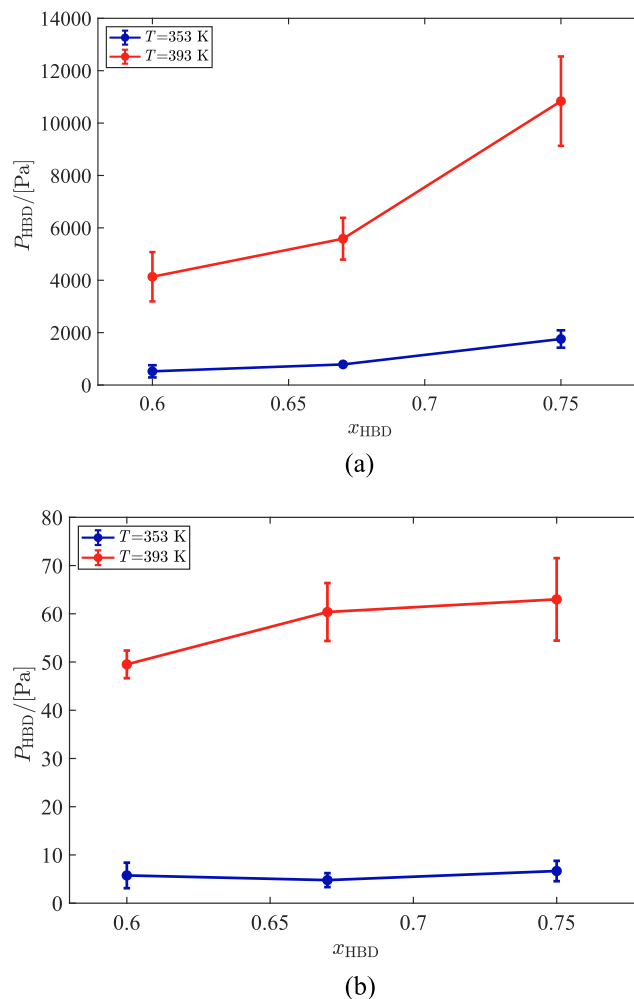
liquid phase simulations in the *NPT* ensemble. The results are presented in Fig. 2, for ChClEg at 353 K and ChClU at 393 K. It can be observed in Fig. 2 that the density of ChClU increases significantly by increasing the mole fraction of the HBD (urea). This is consistent with the findings of Celebi *et al.*[14] from MD simulations (using the same force field) and is possibly due to the larger (experimental) density of pure urea (~1335 kg m^{-3} at room conditions), compared to that of pure choline chloride (~1024 kg m^{-3} at room conditions). At an HBD mole fraction of 0.67 (1:2 M ratio), the density of ChClU is found to be overestimated in the simulations (by 2.8%) with respect to the (extrapolated) experimental value reported by Yadav and Pandey[78] at the same temperature. This overestimation has also been observed in MD studies of ChClU with the same force field parameters[34,38] and is not considered significant. To the best of our knowledge, no experimental data are available for the density of ChClU at other compositions. For ChClEg, the simulation results indicate a negligible effect of the mole fraction of ethylene glycol on the liquid density. Such insensitivity of the density of ChClEg with respect to the composition has also been experimentally observed by Abbott *et al.*[79] at 293 K, although in that study, the density of ChClEg was shown to slightly decrease as the mole fraction of ethylene glycol was increased. The small influence of the liquid composition on the density of ChClEg can be explained by the relatively close values of the densities of pure choline chloride (~1024 kg m^{-3} at room conditions) and pure ethylene glycol (~1113 kg m^{-3} at room conditions). As shown in Fig. 2, the computed density of ChClEg is in excellent agreement with the experimental value reported by Yadav *et al.*[80] at the HBD mole fraction of 0.67. As for ChClU, to the best of our knowledge, no experimental data are available for the density of ChClEg at other compositions at the temperatures considered in this work. Similar results were obtained for the densities of ChClEg and ChClU at other temperatures, as presented in Fig. S6 in the supplementary material. The difference between the computed density of ChClU and the experimental value increases with an increase in temperature, i.e., 3.9% relative deviation at 433 K

FIG. 2. Computed liquid densities of ChClEg (at 353 K) and ChClU (at 393 K) as a function of the mole fraction of the HBD component (ethylene glycol or urea) in the liquid phase. The solid lines are drawn to guide the eye. The experimental data in studies by Yadav and Pandey[78] (for ChClU) and Yadav *et al.*[80] (for ChClEg) are also shown for comparison.

compared to 2.8% at 393 K, indicating the reduced suitability of the used force field parameters at higher temperatures. For ChClEg, the excellent agreement between the computed density and the experimental measurement is maintained at the higher temperature of 393 K (Fig. S6). It is important to note that for achieving a better agreement between the computed densities of ChClU and experimental data, the force field parameters would need to be refined. This would possibly result in an increase in the computed vapor pressures of ChClU and the partial pressures of its components (listed in Tables I and II) due to the weakening of the intermolecular forces at a reduced density. Furthermore, the charge scaling factors used for the cation and anion were originally obtained based on the properties of ChClU and ChClEg, with a HBA:HBD molar ratio of 1:2. This means that the accuracy of the models may be compromised at other liquid compositions. However, due to the lack or scarcity of experimental data for these DESs at other compositions, it is currently not possible to fine tune the existing force field parameters.

The computed partial pressures of the HBD components of ChClEg (ethylene glycol) and ChClU (urea) are presented in Fig. 3, as a function of the liquid phase mole fraction of the HBD. As can be observed in Fig. 3(a), with an increase in x_{HBD} from 0.6 to 0.75, the partial pressure of ethylene glycol increases significantly: from 523 to 1757 Pa, at 353 K, and from 4133 to 10 837 Pa, at 393 K. In sharp contrast, the partial pressures of urea only slightly increase with an increase in x_{HBD} from 0.6 to 0.75. These variations in the partial pressure of urea, however, fall within the uncertainty limits (shown with error bars in Fig. 3). Considering the small differences in the values of x_{HBD}, such small changes in the partial pressure of urea imply the insensitivity of its activity coefficient, and thus nonideality, toward the liquid phase composition [based on Eq. (7)], within the studied range of x_{HBD} values. This is consistent with the MD simulation results obtained by Celebi et al.,[14] where a nonideal behavior, quantified by the so-called thermodynamic factor[81] $\Gamma = 1 + (\partial \ln \gamma_1 / \partial \ln x_1)_{T,P}$, was observed for ChClU (with the same force field parameters as used here), and this non-ideality was found to be only slightly affected by the liquid phase mole fraction of urea. It is possible that increasing the concentration of ethylene glycol largely disrupts the hydrogen bond network of ChClEg, resulting in an increase in the vapor pressure, whereas the hydrogen bonding network of ChClU is retained or restructured (and the vapor pressure is not considerably changed) when the urea content is increased. A detailed comparison of the two systems by hydrogen bond analysis is required to corroborate this.[14,33–35] The influence of the liquid phase composition on the partial pressures of choline chloride in both DESs is presented in Fig. S7 in the supplementary material. Despite the slight decrease in the average partial pressure of choline chloride at higher HBD mole fractions (except in ChClEg at 353 K), the differences generally fall within the uncertainty limits, implying a negligible influence of the liquid composition on the partial pressure of choline chloride. For future research, it is recommended to compute the partial pressures over a wider range of HBD mole fractions, where the differences in the partial pressures may become more conspicuous. One should, however, be cautious when considering larger deviations from the eutectic molar ratio, as transition to the solid phase may occur for either of the components. Therefore, it may be necessary to consider higher temperatures for such computations. Additionally, as explained earlier, the accuracy
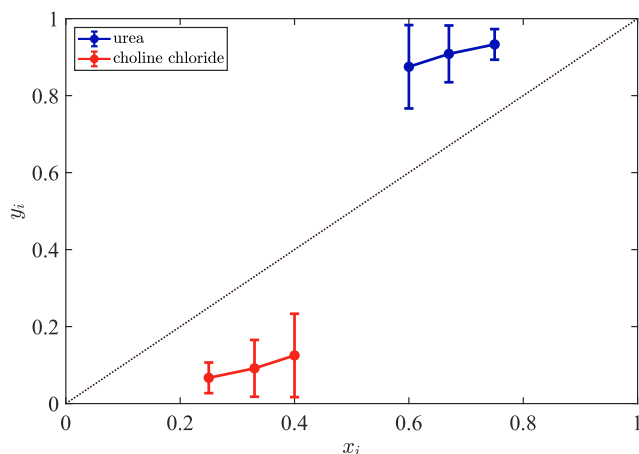

(a)

(b)

FIG. 3. Computed partial pressures of (a) ethylene glycol in ChClEg and (b) urea in ChClU, at various temperatures, as a function of the liquid phase mole fraction of the HBD component (ethylene glycol or urea). The solid lines are drawn to guide the eye.

of the force field may be reduced at larger deviations from the molar ratio for which the optimal force field parameters were obtained (most often the eutectic ratio).

The y–x phase diagram, i.e., the vapor phase mole fraction as a function of the liquid phase mole fraction, is presented in Fig. 4 for the ChClU components at 393 K. It can be observed that at all the liquid compositions, a considerable amount of choline chloride (7%–12%, mole fraction-based) is present in the vapor phase. As expected, by increasing the urea content in the liquid phase, the average vapor phase mole fraction of choline chloride decreases, while that of urea increases, with slopes of less than unity for both components. Similar values and trends were observed for the vapor phase composition at 433 K, as provided in Fig. 8 in the supplementary material. At both temperatures, the variations in the vapor phase composition with the liquid phase mole fraction of urea fall within the uncertainty limits. The relative volatility of urea with respect to

FIG. 4. Computed vapor phase mole fraction of each component i (urea or choline chloride) of ChClU as a function of its mole fraction in the liquid phase at 393 K. The solid lines connecting the data points are drawn to guide the eye. The black dotted line denotes $y_i = x_i$.
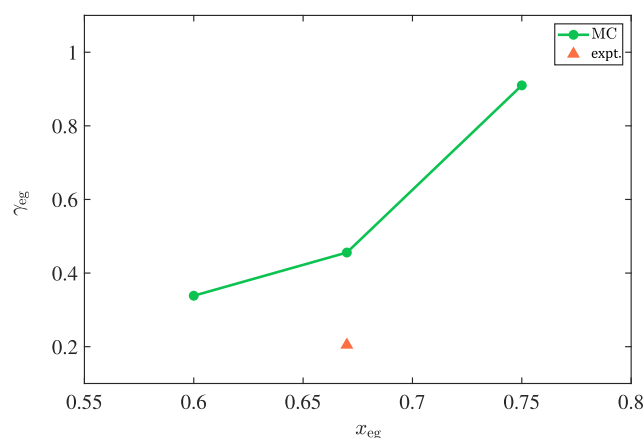
choline chloride, i.e., $\alpha_{ij} = (y_i/x_i)/(y_j/x_j)$ (i and j represent urea and choline chloride, respectively), was computed at 393 K as 4.7, 4.9, and 4.6 at urea mole fractions of 0.6, 0.67, and 0.75, respectively. These values were computed at 433 K as 5.4, 5.6, and 7.6, respectively, indicating an increase in the relative volatility of urea with respect to choline chloride with an increase in temperature, particularly at $x_{HBD} = 0.75$. Although Fig. 4 provides useful information on the phase equilibrium of ChClU, it does not quantify the non-ideality of the mixture. Measurements of the solid–liquid phase equilibrium of ChClU have shown a high non-ideality (with a negative deviation from Raoult's law) for urea and an almost ideal behavior for choline chloride.[9,82] Using the vapor–liquid equilibrium, the non-ideality of real mixtures can be evaluated by computing the activity coefficients of the mixture components from the modified Raoult law [Eq. (7)]. However, as explained in Sec. II, pure urea and pure choline chloride are solids at the temperatures considered in this work. As a result, the pure component vapor pressures (P^{sat}) and thus the activity coefficients could not be calculated from the simulations.

To study the non-ideality of ChClEg, the vapor pressure of pure (liquid) ethylene glycol was computed at 353 K using the same force field parameters as in ChClEg. The vapor pressure of pure ethylene glycol was computed as ~2575 Pa, a value considerably larger than the experimental value of 676 Pa, as reported by Verevkin.[83] The volatility of pure ethylene glycol is therefore overestimated with the GAFF force field parameters used in this work. The computed density of pure ethylene glycol (~1070 kg m^{-3}) is, nonetheless, in close agreement (1.5% relative deviation) with the experimental value reported by Skylogianni et al.[84] (1087 kg m^{-3}). The activity coefficient of ethylene glycol in ChClEg was computed using Eq. (7) from the obtained vapor pressures in pure form and in the DES mixture. For comparison, the experimental activity coefficient of ethylene glycol in ChClEg was computed based on the vapor pressure data in studies by Verevkin[83] (for pure ethylene glycol) and Ravula et al.[23] (for ChClEg), assuming the vapor phase of ChClEg to be entirely composed of ethylene glycol (as supported by the results in Table I).
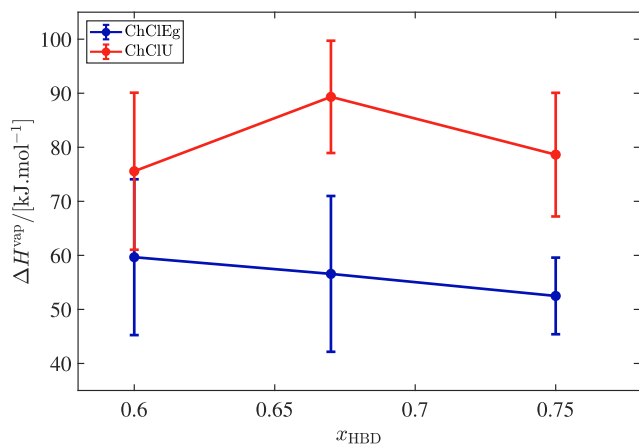
The activity coefficient results are presented in Fig. 5 for various liquid phase mole fractions of ethylene glycol in ChClEg. While the computed vapor pressures of both pure ethylene glycol and ChClEg are overestimated compared to the experimental measurements, the calculated activity coefficient (proportional to the ratio of these vapor pressures, assuming $y_{eg} = 1$ in ChClEg) at the HBD mole fraction of 0.67 is in reasonable agreement with the experimental value. The obtained activity coefficient of ethylene glycol in ChClEg from the simulations sharply increases with an increase in the liquid phase mole fraction of ethylene glycol since at the higher ethylene glycol mole fractions, the liquid composition of the DES approaches that of pure ethylene glycol. Therefore, at the liquid phase mole fractions of 0.6 and 0.67, ethylene glycol shows a non-ideal behavior with large negative deviations from Raoult's law, while at the mole fraction of 0.75, it exhibits an almost ideal behavior. This increase in the activity coefficient of ethylene glycol in ChClEg is the main contributor to the drastic increase in its partial pressure at higher liquid phase mole fractions [Fig. 3(a)].

The enthalpies of vaporization were also computed at different liquid phase compositions. The results are presented in Fig. 6 for both DESs. It can be observed that the differences in the enthalpies of vaporization at the various mole fractions of the HBD lie within the error bars (standard deviations). The error bars were calculated based on the propagation of errors of the corresponding partial pressures. The computed enthalpies of vaporization are thus insensitive to composition changes within the considered range. The computation of the enthalpies of vaporization can be improved by lowering the uncertainty of data at each vapor pressure point (e.g., by longer simulations) and by increasing the number of temperature points to be used in Eq. (8).

Overall, the GAFF force field performs reasonably well regarding the computation of the vapor pressures and enthalpies of vaporization of the DESs, although a larger amount of experimental data is required for a more precise comparison. The focus of the present work was to apply thermodynamic integration to compute the vapor pressures and vapor phase compositions with high precision and

FIG. 5. Computed activity coefficients of ethylene glycol (denoted by "eg") in ChClEg at 353 K, as a function of the mole fraction of ethylene glycol in the liquid phase of the DES, compared with the value obtained from experimental data.[23,83] The solid line is drawn to guide the eye.

FIG. 6. Computed enthalpies of vaporization of ChClEg and ChClU as a function of the liquid phase mole fraction of the HBD component (ethylene glycol or urea). The enthalpies of vaporization were obtained by fitting the Clausius–Clapeyron relation [Eq. (8)] to the computed vapor pressures in temperature ranges of 353–393 K for ChClEg and 393–433 K for ChClU. The solid lines are drawn to guide the eye.

identify trends as a function of the liquid phase composition using the best available force field. It would be interesting in the future to study the influence of the force field parameters and, in particular, the charge scaling value on the accuracy of the computed properties. Based on the small values of the standard deviations reported here, i.e., average standard deviations of 1.5 kJ mol^{-1} for the liquid phase excess Gibbs energies and 174 Pa for partial pressures, thermodynamic integration is a reliable method for the study of the vapor–liquid phase equilibrium of DESs. This method is therefore recommended for the computation of the vapor pressures, vapor phase compositions, and enthalpies of vaporization of other DESs, for which the values of these properties are unavailable or scarce in the literature. It is important to note that the computations in this work were carried out at high temperatures, where the viscosities of the DESs are relatively low, i.e., below 9 cP for ChClU[78] and below 5 cP for ChClEg.[85] Therefore, the equilibration of the system is relatively fast, and sufficient sampling can be performed for the computation of the excess Gibbs energy. These computations would become much more challenging at lower temperatures, where the viscosities of the DESs are exponentially larger, and the equilibration and sampling efficiencies are deteriorated. An alternative approach for the low temperature computations would therefore be to obtain the vapor pressures at high temperatures and use the Clausius–Clapeyron relation [Eq. (8)] or other correlations[22] to extrapolate the vapor pressures to lower temperatures.

IV. CONCLUSIONS

The excess Gibbs energies, vapor pressures, and vapor phase compositions of ChClEg and ChClU DESs were computed at various temperatures from MC simulations using thermodynamic integration. Based on the obtained vapor pressures, the enthalpies of vaporization were calculated and compared with the scarce experimental data available in the literature. The influence of the liquid composition of the DESs on the computed properties was studied by considering the different HBA:HBD molar ratios (or HBD mole

fractions) of 1:1.5, 1:2, and 1:3. For ChClU, the computed vapor pressure and enthalpy of vaporization were in reasonable agreement with experimental data. For ChClEg, the computed enthalpy of vaporization was in excellent agreement with the experimental value, while the vapor pressure was considerably overestimated in the simulations. The computed vapor pressures of both DESs were larger than those of common ILs as reported in the literature. Based on the computations of the vapor pressures and enthalpies of vaporization, the GAFF force field performed reasonably well. The inconsistencies of the experimental data, however, hindered a precise comparison with our simulation results. The computed partial pressures indicated a much larger volatility of ethylene glycol in ChClEg, compared to that of choline chloride, causing the vapor phase of ChClEg to consist entirely of ethylene glycol. For ChClU, small amounts of choline chloride (7%–12% mole fraction-based) were present in the vapor phase. The density of ChClU was found to significantly increase as the mole fraction of urea in the liquid phase was increased, whereas the density of ChClEg was not considerably influenced by the mole fraction of ethylene glycol in the liquid phase. The computed partial pressure of ethylene glycol in ChClEg increased with an increase in its liquid phase mole fraction, while the partial pressure of urea in ChClU and the partial pressures of choline chloride in both DESs were relatively insensitive to the liquid phase composition. As expected, the average vapor phase mole fractions of both components of ChClU slightly increased with an increase in the corresponding liquid phase mole fractions. The computed vaporization enthalpies of both DESs were not considerably affected by the liquid phase compositions. The non-ideal behavior of ethylene glycol in ChClEg was evaluated by computing activity coefficients. It was observed that consistent with experimental data, ethylene glycol exhibited a non-ideal behavior, with negative deviations from Raoult's law, particularly at the lower liquid phase mole fractions. The combination of force field-based MC simulations and thermodynamic integration was shown to be suitable for the computation of the vapor–liquid phase equilibrium of DESs.

SUPPLEMENTARY MATERIAL

See the supplementary material for the molecular structures and force field parameters of the studied DESs as well as additional simulation details and results.

DATA AVAILABILITY

The data that support the findings of this study are available within the article and its supplementary material.

REFERENCES

[1] Q. Zhang, K. De Oliveira Vigier, S. Royer, and F. Jérôme, Chem. Soc. Rev. **41**, 7108 (2012).

[2] E. L. Smith, A. P. Abbott, and K. S. Ryder, Chem. Rev. **114**, 11060 (2014).

[3] D. J. G. P. van Osch, C. H. J. T. Dietz, S. E. E. Warrag, and M. C. Kroon, ACS Sustainable Chem. Eng. **8**, 10591 (2020).

[4] S. Sarmad, Y. Xie, J. P. Mikkola, and X. Ji, New J. Chem. **41**, 290 (2016).

[5] Y. Marcus, *Deep Eutectic Solvents* (Springer International Publishing, Cham, Switzerland, 2019), Vol. 1.

[6] M. Francisco, A. van den Bruinhorst, and M. C. Kroon, Angew. Chemie., Int. Ed. **52**, 3074 (2013).

[7] B. B. Hansen, S. Spittle, B. Chen, D. Poe, Y. Zhang, J. M. Klein, A. Horton, L. Adhikari, T. Zelovich, B. W. Doherty, B. Gurkan, E. J. Maginn, A. Ragauskas, M. Dadmun, T. A. Zawodzinski, G. A. Baker, M. E. Tuckerman, R. F. Savinell, and J. R. Sangoro, Chem. Rev. **121**, 1232 (2021).

[8] D. O. Abranches, M. A. R. Martins, L. P. Silva, N. Schaeffer, S. P. Pinho, and J. A. P. Coutinho, Chem. Commun. **55**, 10253 (2019).

[9] M. A. R. Martins, S. P. Pinho, and J. A. P. Coutinho, J. Solution Chem. **48**, 962 (2019).

[10] A. Jani, B. Malfait, and D. Morineau, J. Chem. Phys. **154**, 164508 (2021).

[11] S. Amara, W. Zaidi, L. Timperman, G. Nikiforidis, and M. Anouti, J. Chem. Phys. **154**, 164708 (2021).

[12] H. Zhang, X. Lu, L. González-Aguilera, M. L. Ferrer, F. del Monte, and M. C. Gutiérrez, J. Chem. Phys. **154**, 184501 (2021).

[13] S. Miao, H. J. Jiang, S. Imberti, R. Atkin, and G. Warr, J. Chem. Phys. **154**, 214504 (2021).

[14] A. T. Celebi, N. Dawass, O. A. Moultos, and T. J. H. Vlugt, J. Chem. Phys. **154**, 184502 (2021).

[15] H. S. Salehi, A. T. Celebi, T. J. H. Vlugt, and O. A. Moultos, J. Chem. Phys. **154**, 144502 (2021).

[16] A. Triolo, M. E. Di Pietro, A. Mele, F. Lo Celso, M. Brehm, V. Di Lisio, A. Martinelli, P. Chater, and O. Russina, J. Chem. Phys. **154**, 244501 (2021).

[17] D. Dhingra, V. Khokhar, S. Juneja, and S. Pandey, J. Chem. Phys. **154**, 164513 (2021).

[18] D. Reuter, P. Münzner, C. Gainaru, P. Lunkenheimer, A. Loidl, and R. Böhmer, J. Chem. Phys. **154**, 154501 (2021).

[19] R. Paul, A. Mitra, and S. Paul, J. Chem. Phys. **154**, 244504 (2021).

[20] A. Paiva, R. Craveiro, I. Aroso, M. Martins, R. L. Reis, and A. R. C. Duarte, ACS Sustainable Chem. Eng. **2**, 1063 (2014).

[21] C. H. J. T. Dietz, J. T. Creemers, M. A. Meuleman, C. Held, G. Sadowski, M. van Sint Annaland, F. Gallucci, and M. C. Kroon, ACS Sustainable Chem. Eng. **7**, 4047 (2019).

[22] K. Shahbaz, F. S. Mjalli, G. Vakili-Nezhaad, I. M. AlNashef, A. Asadov, and M. M. Farid, J. Mol. Liq. **222**, 61 (2016).

[23] S. Ravula, N. E. Larm, M. A. Mottaleb, M. P. Heitz, and G. A. Baker, ChemEngineering **3**, 42 (2019).

[24] C. H. J. T. Dietz, A. Erve, M. C. Kroon, M. van Sint Annaland, F. Gallucci, and C. Held, Fluid Phase Equilib. **489**, 75 (2019).

[25] F. Lima, C. H. J. T. Dietz, A. J. D. Silvestre, L. C. Branco, J. Canongia Lopes, F. Gallucci, K. Shimizu, C. Held, and I. M. Marrucho, J. Phys. Chem. B **124**, 10386 (2020).

[26] A. Boisset, J. Jacquemin, and M. Anouti, Electrochim. Acta **102**, 120 (2013).

[27] S.-H. Wu, A. R. Caparanga, R. B. Leron, and M.-H. Li, Thermochim. Acta **544**, 1 (2012).

[28] K. Xin, I. Roghair, F. Gallucci, and M. van Sint Annaland, J. Mol. Liq. **325**, 115227 (2021).

[29] J. Gross and G. Sadowski, Ind. Eng. Chem. Res. **40**, 1244 (2001).

[30] A. Klamt, J. Phys. Chem. **99**, 2224 (1995).

[31] T. Aissaoui, I. M. AlNashef, and Y. Benguerba, J. Nat. Gas Sci. Eng. **30**, 571 (2016).

[32] H. S. Salehi, M. Ramdin, O. A. Moultos, and T. J. H. Vlugt, Fluid Phase Equilib. **497**, 10 (2019).

[33] E. S. C. Ferreira, I. V. Voroshylova, C. M. Pereira, and M. N. D. S. Cordeiro, J. Phys. Chem. B **120**, 10124 (2016).

[34] S. L. Perkins, P. Painter, and C. M. Colina, J. Phys. Chem. B **117**, 10250 (2013).

[35] S. L. Perkins, P. Painter, and C. M. Colina, J. Chem. Eng. Data **59**, 3652 (2014).

[36] B. Doherty and O. Acevedo, J. Phys. Chem. B **122**, 9982 (2018).

[37] J. Wang, R. M. Wolf, J. W. Caldwell, P. A. Kollman, and D. A. Case, J. Comput. Chem. **25**, 1157 (2004).

[38] A. T. Celebi, T. J. H. Vlugt, and O. A. Moultos, J. Phys. Chem. B **123**, 11014 (2019).

[39] H. S. Salehi, R. Hens, O. A. Moultos, and T. J. H. Vlugt, J. Mol. Liq. **316**, 113729 (2020).

[40] C. I. Bayly, P. Cieplak, W. Cornell, and P. A. Kollman, J. Phys. Chem. **97**, 10269 (1993).

[41] F.-Y. Dupradeau, A. Pigache, T. Zaffran, C. Savineau, R. Lelong, N. Grivel, D. Lelong, W. Rosanski, and P. Cieplak, Phys. Chem. Chem. Phys. **12**, 7821 (2010).

[42] H. Liu, E. Maginn, A. E. Visser, N. J. Bridges, and E. B. Fox, Ind. Eng. Chem. Res. **51**, 7242 (2012).

[43] C. I. Bayly, K. M. Merz, D. M. Ferguson, W. D. Cornell, T. Fox, J. W. Caldwell, P. A. Kollman, P. Cieplak, I. R. Gould, and D. C. Spellmeyer, J. Am. Chem. Soc. **117**, 5179 (1995).

[44] D. Frenkel and B. Smit, *Understanding Molecular Simulation: From Algorithms to Applications*, 2nd ed. (Academic Press, San Diego, CA, 2002), Vol. 1.

[45] P. P. Ewald, Ann. Phys. **369**, 253 (1921).

[46] M. P. Allen and D. J. Tildesley, *Computer Simulation of Liquids*, 2nd ed. (Oxford University Press, Inc., New York, NY, 2017).

[47] R. Hens, A. Rahbari, S. Caro-Ortiz, N. Dawass, M. Erdős, A. Poursaeidesfahani, H. S. Salehi, A. T. Celebi, M. Ramdin, O. A. Moultos, D. Dubbeldam, and T. J. H. Vlugt, J. Chem. Inf. Model. **60**, 2678 (2020).

[48] .H. M. Polat, H. S. Salehi, R. Hens, D. O. Wasik, F. de Meyer, C. Houriez, C. Coquelet, S. Calero, D. Dubbeldam, O. A. Moultos, and T. J. H. Vlugt, J. Chem. Inf. Model. **61**, 3752 (2021).

[49] A. Rahbari, R. Hens, M. Ramdin, O. A. Moultos, D. Dubbeldam, and T. J. H. Vlugt, Mol. Simul. **47**, 804 (2021).

[50] W. Shi and E. J. Maginn, J. Chem. Theory Comput. **3**, 1451 (2007).

[51] W. Shi and E. J. Maginn, J. Comput. Chem. **29**, 2520 (2008).

[52] T. W. Rosch and E. J. Maginn, J. Chem. Theory Comput. **7**, 269 (2011).

[53] A. Poursaeidesfahani, A. Torres-Knoop, D. Dubbeldam, and T. J. H. Vlugt, J. Chem. Theory Comput. **12**, 1481 (2016).

[54] A. Poursaeidesfahani, R. Hens, A. Rahbari, M. Ramdin, D. Dubbeldam, and T. J. H. Vlugt, J. Chem. Theory Comput. **13**, 4452 (2017).

[55] N. Dawass, R. R. Wanderley, M. Ramdin, O. A. Moultos, H. K. Knuutila, and T. J. H. Vlugt, J. Chem. Eng. Data **66**, 524 (2021).

[56] A. Rahbari, R. Hens, D. Dubbeldam, and T. J. H. Vlugt, Mol. Phys. **117**, 3493 (2019).

[57] A. Rahbari, J. Brenkman, R. Hens, M. Ramdin, L. J. P. van den Broeke, R. Schoon, R. Henkes, O. A. Moultos, and T. J. H. Vlugt, J. Chem. Eng. Data **64**, 4103 (2019).

[58] K. R. J. Lovelock and R. Soc, Open Sci. **4**, 171223 (2017).

[59] N. Rai and E. J. Maginn, J. Phys. Chem. Lett. **2**, 1439 (2011).

[60] S. P. Verevkin, D. H. Zaitsau, V. N. Emel'yanenko, A. V. Yermalayeu, C. Schick, H. Liu, E. J. Maginn, S. Bulut, I. Krossing, and R. Kalb, J. Phys. Chem. B **117**, 6473 (2013).

[61] S. D. Chambreau, G. L. Vaghjiani, A. To, C. Koh, D. Strasser, O. Kostko, and S. R. Leone, J. Phys. Chem. B **114**, 1361 (2010).

[62] D. H. Zaitsau, R. Siewert, A. A. Pimerzin, M. Bülow, C. Held, S. Loor, S. Schulz, and S. P. Verevkin, J. Mol. Liq. **323**, 114998 (2021).

[63] D. Strasser, F. Goulay, M. S. Kelkar, E. J. Maginn, and S. R. Leone, J. Phys. Chem. A **111**, 3191 (2007).

[64] A. Rahbari, R. Hens, O. A. Moultos, D. Dubbeldam, and T. J. H. Vlugt, J. Chem. Theory Comput. **16**, 1757 (2020).

[65] A. Rahbari, J. C. Garcia-Navarro, M. Ramdin, L. J. P. van den Broeke, O. A. Moultos, D. Dubbeldam, and T. J. H. Vlugt, J. Chem. Eng. Data **66**, 2071 (2021).

[66] T. I. Morrow and E. J. Maginn, J. Phys. Chem. B **106**, 12807 (2002).

[67] D. Kussainova, A. Mondal, J. M. Young, S. Yue, and A. Z. Panagiotopoulos, J. Chem. Phys. **153**, 024501 (2020).

[68] N. Dawass, P. Krüger, S. K. Schnell, J.-M. Simon, and T. J. H. Vlugt, Fluid Phase Equilib. **486**, 21 (2019).

[69] J. M. Smith, H. C. Van Ness, and M. Abbott, *Introduction to Chemical Engineering Thermodynamics*, 7th ed. (McGraw-Hill, New York, NY, 2005).

[70] A. Z. Panagiotopoulos, J. Chem. Phys. **153**, 010903 (2020).

[71] D. R. Lide, *CRC Handbook of Chemistry and Physics*, 85th ed. (CRC Press, Boca Raton, FL, 2004).

[72] D. Zaitsau, G. J. Kabo, A. A. Kozyro, and V. M. Sevruk, Thermochim. Acta **406**, 17 (2003).

[73] M. J. Moran, H. N. Shapiro, D. D. Boettner, and M. B. Bailey, *Fundamentals of Engineering Thermodynamics*, 8th ed. (John Wiley & Sons, New York, NY, 2014).

[74] O. Aschenbrenner, S. Supasitmongkol, M. Taylor, and P. Styring, Green Chem. **11**, 1217 (2009).

[75] T. Köddermann, D. Paschek, and R. Ludwig, ChemPhysChem **8**, 2464 (2007).

[76] S. V. Sambasivarao and O. Acevedo, J. Chem. Theory Comput. **5**, 1038 (2009).

[77] N. Rai and E. J. Maginn, Faraday Discuss. **154**, 53 (2012).

[78] A. Yadav and S. Pandey, J. Chem. Eng. Data **59**, 2221 (2014).

[79] A. P. Abbott, G. Capper, D. L. Davies, R. K. Rasheed, and V. Tambyrajah, Chem. Commun. **2003**, 70.

[80] A. Yadav, J. R. Kar, M. Verma, S. Naqvi, and S. Pandey, Thermochim. Acta **600**, 95 (2015).

[81] R. Taylor and H. A. Kooijman, Chem. Eng. Commun. **102**, 87 (1991).

[82] L. J. B. M. Kollau, M. Vis, A. van den Bruinhorst, A. C. C. Esteves, and R. Tuinier, Chem. Commun. **54**, 13351 (2018).

[83] S. P. Verevkin, Fluid Phase Equilib. **224**, 23 (2004).

[84] E. Skylogianni, R. R. Wanderley, S. S. Austad, and H. K. Knuutila, J. Chem. Eng. Data **64**, 5415 (2019).

[85] A. R. Harifi-Mood and R. Buchner, J. Mol. Liq. **225**, 689 (2017).